Research Article   **Open Access**

Design, Modeling and Development of a Serial Hybrid Motorcycle with HCCI Engine

Yuh-Yih Wu[1], Chen Duan[2], Kai-Xian Hong[1], Hsien-Chi Tsai[1] and Craig J Hoff[2]*

[1]Department of Vehicle Engineering, National Taipei University of Technology, Sec.3, Zhongxiao E.Rd., Taipei 10608, Taiwan
[2]Department of Mechanical Engineering, Kettering University, USA

Abstract

This paper discusses the design, modeling, and development of small motorcycle equipped with a HCCI engine in a series hybrid configuration. A mathematical model was developed using MATLAB/Simulink and used to size the powertrain components and to predict fuel economy. A conventional 125 cc spark ignition engine was modified to run in HCCI combustion mode and integrated into a prototype vehicle. Dual-fuel and external EGR strategies were used to upgrade the engine speed and torque capabilities of the engine to meet the requirements of the powertrain. An electrical generator, hub-motor, battery pack and other power electronics devices were used to form the electrical system for the vehicle. The advantages of the proposed design compared to the original motorcycle with SI engine and CVT transmission are: 1) a reduction in noxious emissions due to the HCCI combustion, and 2) higher fuel economy in city driving because of the HCCI engine and series hybrid powertrain. Fuel economy was measured by driving the motorcycle on a chassis dynamometer using a sequence of ECE-40 driving cycles. The overall fuel economy was measured to be 73.7 km/L which represents a 139.3% increase in fuel economy over the baseline vehicle.

Keywords: Hybrid motor cycle; HCCI engine; Battery; Fuel feed system

Introduction

Lead by booming economies in China, India, and the Middle East, global energy demand is projected to increase by one-third by 2035 [1]. A significant portion of this increase is being driven by increased demand for fossil fuels in the transportation sector. Governments and automakers in many countries have responded by allocating considerable economic resources to develop renewable fuels and fuel efficient vehicle powertrain technologies [2]. In the international market, Electric Vehicles (EVs) and Electric Motorcycles (EMs), which have the potential to reduce fossil fuel usage, are facing challenges in consumer acceptance due to range limitations, lack of charging stations, the high cost of batteries and poor battery performance [3]. Hybrid Electric Vehicles (HEVs), which combine the advantages of internal combustion engines and electric motors using efficient energy management strategies, are capable a meetings consumer expectations while increasing fuel economy and decreasing emissions.

Currently, both gasoline Spark Ignition (SI) and diesel Compression Ignition (CI) engines have been integrated into hybrid powertrains. CI engines have a higher thermal efficiency than SI engines, due to the higher compression ratios and lean burn ratios used. But in conventional CI engines the air/fuel charge is not pre-mixed, which leads to incomplete combustion and very high temperatures in the combustion zones. This then results in high levels of NOx and Particulate Matter (PM) emissions. SI engines, which use homogeneous (pre-mixed) air/fuel charges and near stoichiometric air/fuel ratios, produce much lower NOx and PM emissions. However, SI engines have lower thermal efficiencies than CI engines due to the lower compression ratios used to prevent engine knock and throttling losses during Partial Open Throttle (POT) operation.

Homogeneous Charge Compression Ignition (HCCI) engines combine the advantages of both SI and CI engines. The direct injection used in HCCI engines allows higher compression ratios to be used than in conventional SI engines, which improves efficiency to levels comparable to CI engines. The very lean homogeneous air/fuel charge

in the HCCI engine is burned volumetrically, which greatly reduces the in-cylinder temperature and in turn greatly reducing the production of NOx. The charge is also sufficiently well-mixed to reduce the production of soot (PM). A difficulty with HCCI engines is controlling the combustion process to allow HCCI operation over a wide range of speeds and loads [4].

In a series hybrid powertrain, the internal combustion engine is typically run at a constant speed to drive the generator. This makes it is possible to utilize HCCI engine in series hybrid powertrain, because it is difficult to control the torque and speed of an HCCI engine simultaneously. While integrating the HCCI engine into a serial hybrid powertrain, in order to increase the electrical power generated, the state engine speed and load should be increased. Thus in this research, several methodology are developed. According to the burning characteristics of HCCI engine [5], utilization of mixed fuel and external Exhaust Gas Recirculation (EGR) [6] are realized, then the HCCI state speed and torque can be increased to 3000~4000 rpm and 5 Nm respectively, which upgrades the possibility of utilizing HCCI engine in serial hybrid powertrain.
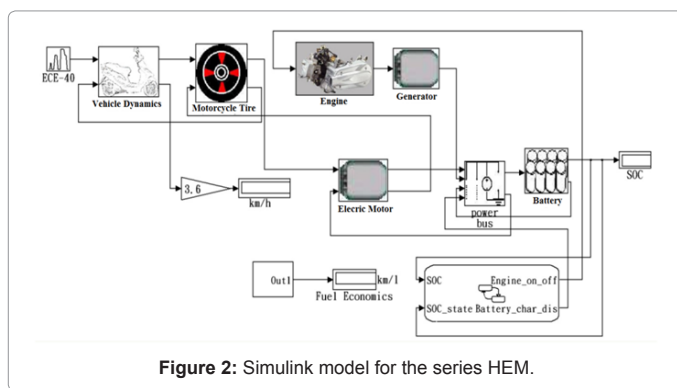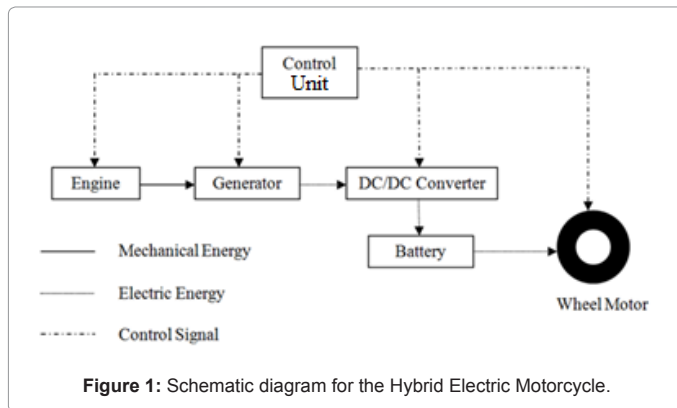
A schematic diagram for the Hybrid Electric Motorcycle (HEM) is shown in Figure 1. The HCCI engine is used to drive an electrical generator. The electric power from the generator is used to charge the battery pack utilizing a DC/DC converter, which boosts the generator output voltage to a level higher than the battery terminal voltage. The wheel motor is driven by the electric power flow from the battery to

---

Figure 1: Schematic diagram for the Hybrid Electric Motorcycle.

Figure 2: Simulink model for the series HEM.

propel the vehicle. The engine combustion and all power flow action are monitored and controlled by an integrated controller.

Modeling and simulation

Prior to building the prototype, a mathematical model of the HEM was developed in order to properly size components and to predict vehicle performance and fuel economy. The model, which is shown in was developed using MATLAB/Simulink using a Backward-Facing approach (Figure 2). Details on the model are explained below.

Vehicle dynamics: In this Backward-Facing model, the controlling input variable is vehicle speed. From the prescribed input speed, the Vehicle Dynamics block calculates the required tractive force for the motorcycle from following equation:

$$F_{req} = R_{acc} + R_g + R_r + R_a$$

Where R_{acc} is the acceleration resistance and defined as:

$$R_{acc} = m_{veh}a = m_{veh}\frac{v_{req} - v_{pre}}{\Delta t}$$

Where m_{veh} is the mass of the motorcycle, V_{reqis} the required velocity at the current time step and V_{pre} is the required velocity from the previous time step.

The grade resistance $R_{g}$is defined as:

$$R_g = m_{veh} \cdot g \cdot Sin\theta$$

Where g is the gravitational constant and θ is the grade angle.

The rolling resistance for the vehicle R_r is defined as:

$$R_r = \mu_r \cdot m_{veh} \cdot Cos\theta$$

Where μ_r is the rolling resistance coefficient and is selected as μ_r= 0.010 in the simulation assuming the vehicle is driving down a good paved road.

The aerodynamic drag R_a is defined as:

$$R_a = \frac{1}{2}\rho_{air} \cdot C_d \cdot A_{veh} \cdot v_{pre}^{\ 2}$$

Where ρ_{air} is the density of air, C_d is the vehicle's drag coefficient and A_{veh} is the front area of the vehicle. All these parameters are defined according to the Sanyang 150 c.c. motorcycle which was the basis for the prototype HEM.

Motorcycle tire: The 'Motorcycle Tire' model is used to evaluate the required speed and torque conditions for the electric wheel motor. The calculation results from Vehicle Dynamic block are sent to Motorcycle Tire block, which calculates the output speed and torque from the following equations:

$$\omega_{drive} = R_{fd} \cdot \frac{60}{2\pi \cdot R_w} \cdot V_{req}$$

$$T_{drive} = T_{req} \cdot r_w \cdot \frac{\eta_{fd}}{R_{fd}}$$

Where r_w is the radius of the wheel, R_{fd} is the final drive ratio, and η_{fd} is the efficiency of the final drive.

Electric motor: In a conventional motorcycle, the internal combustion engine operates at a low efficiency during idling or at low vehicle speed. But for a series HEM the engine is decoupled from the wheels and the engine is only used to run the generator. When the engine is on it is designed to operate at conditions that optimizes the engine's efficiency. Power to drive motorcycle is always delivered via the electric motor. The motor must be sized to meet the vehicle performance needs for the vehicle. For a Backward-Facing simulation there are two limitations on the electric motor: first, the motor speed should not exceed the maximum rated speed for the motor; second, the model output torque should be limited by both the maximum torque output of the motor and the rotational inertia of the driveline. The electric motor model used here can be described with the two following equations.

$$P_{m\_req} = \min\left(P_{m\_map}, I_{bat} \cdot V_{bat}\right)$$

$$P_{m\_map} = f\left(\tau_{m\_lim}, \omega_{m\_lim}\right)$$

Where P_{m_req} is the required power of the motor, P_{m_map} is the possible output power at the operating speed and torque conditions, and the quantity $I_{bat} \oplus V_{bat}$ is the maximum power that be delivered by the battery pack. In the electrical power calculation I_{bat} and V_{bat} are the discharge current and the terminal voltage of the battery, respectively.

P_{m_map} is a function of the operating speed and torque conditions for the motor, which is limited in the following ways:

$$\omega_{m\_lim} = \min\left(\omega_{m\_req}, \omega_{m\_max}\right)$$

$$\tau_{m\_lim} = \min\left[f_1\left(\omega_{m\_lim}\right), \tau_{m\_req} + Jm\left(\frac{\Delta\omega_{m\_lim}}{\Delta t}\right)\right]$$

Where f_1 is the maximum torque function of the electric motor.

Battery: In this model the battery is simulated as a simple RC circuit as shown in Figure 3. The power electronics devices such as the DC/DC converter and the motor controller driving the motor are ignored.

The terminal voltage (V_t) for the battery is found from:

$$V_t = V_{oc} - I_{bat} \cdot R_{\text{int}}$$

Where V_{oc} is open circuit voltage of the battery and R_{int} is the internal resistance of the battery pack. For the estimation of the State of Charge (SOC), a Coulomb Counting method is utilized in the simulation and can be represented as the following equation:

$$SOC = SOC_{\text{int}} - \frac{\int_0^t I_{bat} dt}{Ah}$$

Where SOC_{int} is the initial state of charge before discharging the battery and Ah is the total rated capacity of the battery.

Engine: Based on the estimation of the battery SOC, the starting control strategy of the internal combustion engine is determined. A simple 'thermostat' style control strategy is used in the model; the engine is set to start while the battery SOC is less than 50% and shut down when higher than 90%. The engine in this HEM simulation is modeled using a Brake Specific Fuel Consumption (BSFC) look-up table developed from real test data from the Sanyang 125 c.c. engine and its modified HCCI version. Figure 4 shows the BSFC plot of the original engine in SI mode and target engine in HCCI mode.

Generator and CVT: The generator model is based on data for the Prius permanent magnet generator which was acquired from the ADVISOR software [7]. To scale the generator data for this application, the torque index values were scaled by 1/6 of the original value without
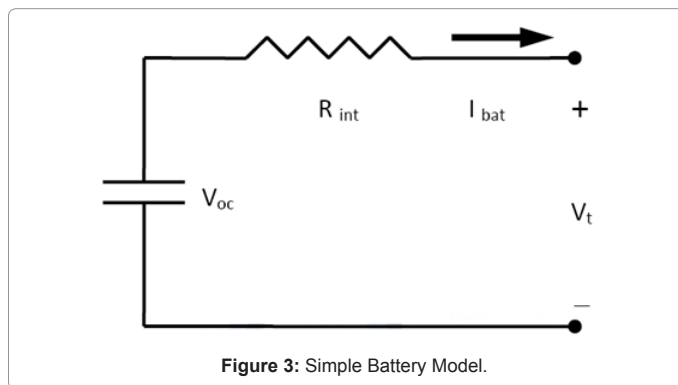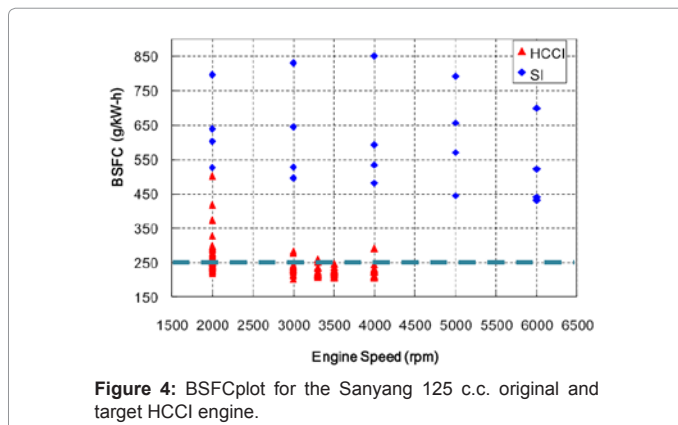

Figure 3: Simple Battery Model.

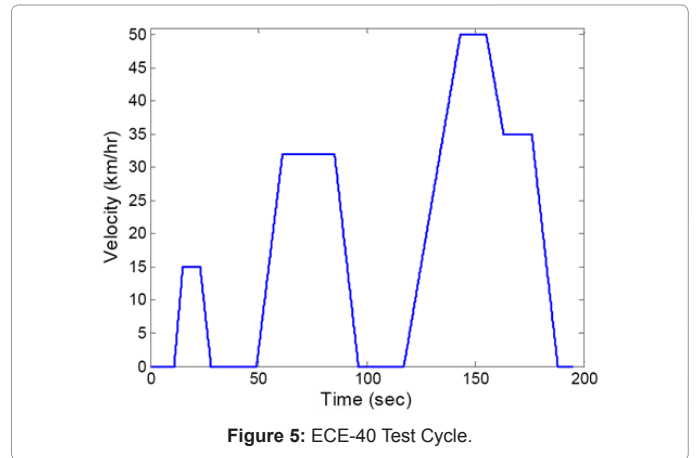**Figure 4:** BSFCplot for the Sanyang 125 c.c. original and target HCCI engine.

Figure 5: ECE-40 Test Cycle.

Powertrain	Fuel Economy (km/L)	Increment Percentage
CVT Transmission	32.61	----
Serial Hybrid System	75.62	132%

Table 1: Simulation Results for CVT and HEM.

changing the speed range and efficiency map. With this scaling the maximum power for the motor is 1000W. In order to compare the fuel economy between the hybrid system and the original Continuously Variable Transmission (CVT) powertrain, A CVT model was also developed. The CVT model is described with the equation below:

$$T_e = T_{req} \cdot \eta_{cvt} \cdot \eta_{CVT}$$

Where T_e is the engine output torque, T_{req} is the required torque of the final drive and n_{CVT}, η_{CVT} are the transmission ratio and mechanical efficiency of CVT respectively.

Simulation Results

Both the HEM and conventional CVT model were run with the ECE-40 test cycle as the speed input. Figure 5 shows the vehicle speed history for the ECE-40 cycle, which is representative of city road conditions for a motorcycle.

The simulation results for both conventional CVT powertrain and the HEM system are shown in Table 1. It can be observed that the fuel economy of the HEM is increased by 132% from the original CVT motorcycle in city driving (ECE-40). It also means that the components of the HEM can be integrated together to work well, which allow us to develop a prototype of HEM and test it.

HCCI engine development

The HCCI engine developed for this application is based on a 125 c.c. Sanyang SI motorcycle engine. The engine was modified by adding necessary systems such as an engine control unit, Emission Gas Recirculation (EGR) system, etc. The engine can operate in either SI or HCCI combustion mode and utilize alternative fuels. Since it is impossible to operate in HCCI combustion mode from cold starting, the engine is designed to first start in SI combustion mode. When the temperature and pressure inside the cylinder allows for compression ignition the HCCI combustion mode can be switched by the engine control unit.

Fuel feed system

HCCI engines have a narrow range operating conditions which will

allow HCCI combustion. However, engine operating speed and torque will vary during operation. Increasing fuel demand will change the fuel density inside the cylinder and lead to the acceleration of combustion speed, which may damage the engine due to the rapid increases in in-cylinder pressure. Thus for HCCI engine, it is recommended to blend fuel with an additive to help control the spontaneous combustion of the main fuel [6]. Earlier research shows that by blending 92 octane unleaded gasoline with Dimethyl Ether (DME) can make the engine have a very similar Brake Mean Effective Pressure (BMEP) to the original SI engine. In addition, by utilizing an EGR system to widen the operating range, the BSFC of the HCCI engine can achieve less than 250g/kW-h within speeds from 3000rpm to 4000rpm [7].

The modification of the HCCI engine fuel feed system is based on the discussion above. The engine is modified to be a dual-fuel feed system, as shown in Figure 6.

For the dual-fuel feed system, the original gasoline fuel injector is kept to feed the gasoline. The DME fuel injector is added downstream of the gasoline fuel injector. A flow meter is used to measure the DME flow rate and a steel cylinder acting as a plenumis used to stabilize the pressure before injecting. The DME injector is a special injector without rubber material inside because DME can corrode rubber. For the same reason, a Teflon pipe is selected to transport the DME. Figure 7 shows the DME injector as it is installed near the gasoline injector on the intake manifold.
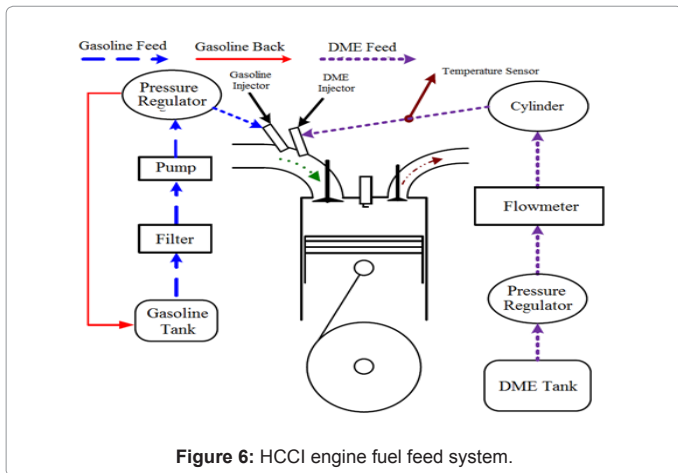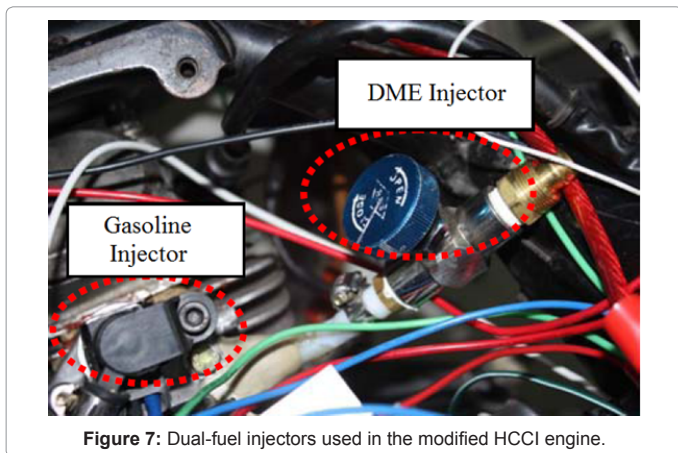

Figure 6: HCCI engine fuel feed system.

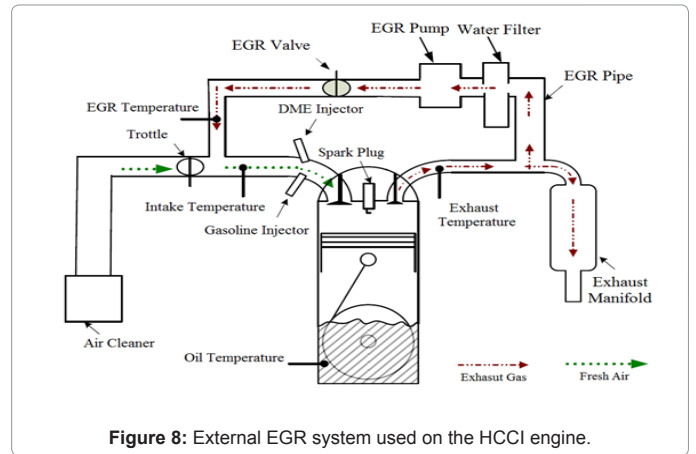**Figure 7:** Dual-fuel injectors used in the modified HCCI engine.

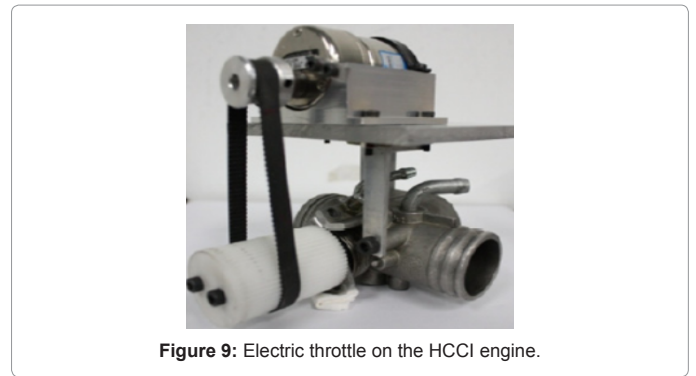**Figure 8:** External EGR system used on the HCCI engine.

Figure 9: Electric throttle on the HCCI engine.

External EGR

The combustion reaction in a HCCI engine has a very high heat release rate, especially when the engine torque increases [8]. In order to widen the operating range of the engine, and at the same time, avoid engine damaging from fast heat release, external EGR system is set up on this HCCI engine. Another advantage of utilizing EGR system is that the production of noxious gases such as NO_x and CO can be reduced due to the reduction of combustion temperature [9]. Figure 8 shows the diagram of the realized external EGR system.

The temperature of exhaust gas is very high, but the temperature inside the EGR system is relatively low. Thus the water vapor in exhaust gas will condense and be drawn to the cylinder, which has negative effects on engine performance. Consequently, a water filter is used. In addition, an EGR pump is used to increase the recycle gas flow and a valve is used to control the EGR percentage. Both the intake and exhaust gas were sampled by HORIBA gas analyzer to calculate the EGR percentage according to the following equation [9].

$$EGR\% = \frac{\left(CO_2\%\right)_{intake}}{\left(CO_2\%\right)_{exhaust}} \times 100\%$$

Electric throttle

During the engine switching process from SI combustion mode to HCCI combustion mode, the action of throttle is very important. This is because during the SI combustion warming up, the throttle is set to part open to make the engine operate at idling speed. However, Wide Open Throttle (WOT) is necessary in the HCCI combustion process. Thus in the modified engine, the original throttle controlled by steel cable is replaced by an electric throttle controlled by ECU. Based on

this, the combustion process can be controlled accurately and throttle angle data can be recorded. Figure 9 shows the electric throttle used on the HCCI engine.

In the electric throttle, the throttle valve is meshed to the control motor by two gears and a rubber chain. The control motor is a stepper motor driven by a Pulse Width Modulated (PWM) signal from the Engine Control Unit (ECU). The throttle angle sensor on engine intake valve measures the throttle percentage and sends it back to ECU to realize feed-back control. By utilizing the electric throttle, much more accurate and rapid control is obtained.

Engine control unit

The Engine Control Unit (ECU) is the core of an engine, which receives measurements from the sensors and process feed-back control to the engine, such as throttle angle, injection and spark timing etc. To realize programmable control and to simultaneously monitor and record data, the original ECU is replaced by Woodward MCS ECU555-80 control unit. This control unit can be connected to a PC and to the CAN bus of a vehicle to link with specific sensors and engine components. With this ECU, it is possible to control all engine actions from a PC. The control code is developed in MATLAB/Simulink Realtime Workshop and burned into the ECU. Figure 10 is a picture of ECU555-80.

Hybrid system integration

After the HCCI engine modifications were completed, the engine along with other series hybrid components (generator, battery and electric motor) was integrated on board a Sanyang 150 c.c. motorcycle, as shown in Figure 11.

A conventional SI engine and a CVT compose the powertrain of the original motorcycle. Besides the modification of the engine discussed in the previous section, the CVT is also removed to build the series hybrid powertrain. But before removing the CVT, the motorcycle was tested on a chassis dynamometer driving an ECE-40 cycle to establish the base-line city fuel economy. Thus a comparison of the fuel economy

Figure 10: Woodward MCS ECU555-80.

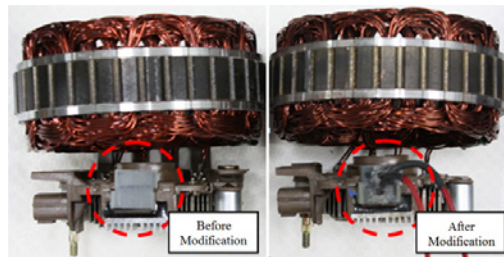**Figure 11:** Sanyang 150 c.c. Motorcycle.

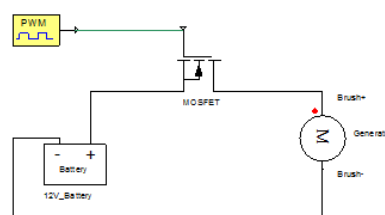**Figure 12:** Generator modifications.

Figure 13: Magnetizing current control circuit.

between the conventional motorcycle and HEM can be made.

Generator: In serial hybrid systems, a generator driven by engine is set to generate electricity to charge the battery. Thus there is no mechanical coupling between the engine and the powertrain. In this motorcycle, a generator whose rated power is 1.5 kW is utilized. The output control for the generator was modified to meet the needs of this HEM application.

In the original generator, there was an Integrated Circuit (IC) regulator to stabilize the output voltage at 13.5V while the rotator speed is varying. But to utilize the generator in the hybrid system, it is necessary to vary the output voltage to fit the needs for battery charging. Also it is important to control the generator magnetizing current, which controls the load on the engine, to make the engine work in a low BSFC operating point at stable speeds. In order to achieve this purpose, the IC regulator is removed and the connectors are insulated to avoid conducting with the brush. Then the brush is connected to a control circuit out of the generator. Figure 12 shows the modification to the generator.

From the figure it can be observed that the brush connects two wires. These two wires are connected to a control circuit between 12V battery and the brush. Figure 13 shows the schematic of the control circuit.

A MOSFET connects the 12V battery and the generator brush. The MOSFET is triggered by the PWM signal from the ECU. By changing the pulse width of the gate driver signal, the average magnetizing current can be changed. Because the magnetizing current actually indicates the resistance to the rotator driven by the engine, the engine load is now controlled by the ECU. After finishing these modifications, the generator is loaded to the motorcycle as shown in Figure 14. The generator rotator is meshed to the engine crankshaft with a belt.

Battery and charging system: The battery pack is the electric energy storage part of a hybrid system. For serial hybrid powertrain, it is recommended to use a battery pack that can be deeply discharged; thus the pure electric mileage of the vehicle can be extended and higher fuel economy can be obtained. For this HEM using an HCCI engine,

Figure 14: Generator is connected to the engine by a belt drive.

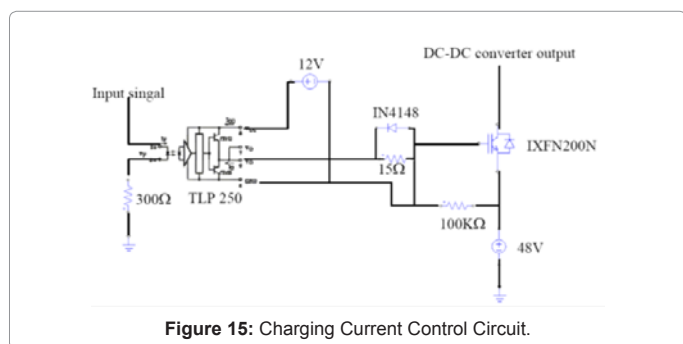| Parameter	Value
Input Voltage	19~72V
Input Current	23.5A/48VDC
Output Voltage	46~60V
Output Current	0~21A
Max Output Power	1008W
Efficiency	90%

Table 2: DC/DC Converter Parameters.

Figure 15: Charging Current Control Circuit.

four YUASA REC22-12 Lead-acid batteries were used with a 12 V rated voltage and 22 Ah rated capacity. Wired in series the pack is rated 48 V voltage and 22 Ah. The 48V pack is sufficient for the electric motor controller which is rated at 30~60 V.

To charge the battery with the generator, a DC/DC converter is needed to regulate the output voltage of the generator to be higher than the battery terminal voltage. And at the same time, the voltage stress due to the generator speed varying should also be compensated by the converter. To achieve these two purposes, a SD-1000L-48 DC/DC converter is selected. The parameters for the converter are shown in Table 2.

When the engine is running at stable speed, the output voltage can be controlled around a constant value. Although there is some voltage change as a result of speed ripple, the input range of the DC/DC converter can handle the variability. The output voltage of the converter is fixed at 52V, thus the 48V battery pack can be charged.

It should be noted that during the charging process, the battery internal resistance will change, and the charging current will decreases as the battery terminal voltage reaches the converter output voltage. Thus an additional circuit is designed to fix the charging current. The schematics of this circuit are shown in Figure 15.

The TLP 250 is an optical coupler to isolate the control and power

parts of the circuit. The IXFN 200 N is a MOSFET between the DC/DC converter and battery terminal. With this circuit, by monitoring the simultaneous charging current and using a feed-back control program in ECU, the charging current can be fixed at 5A. The controlling signal is PWM from ECU, and the charging current is actually determined by the pulse width.

Electric motor: For electrical vehicles, the multi-speed transmission in conventional vehicles is typically replaced by a single-speed transmission or just a final drive. This is because the torque-speed performance of electric motors can fit the road drive requirement better than internal combustion engines. For an electric scooter or HEM, due to the space and weight limitations and also because they have only two wheels, hub motors are highly recommended as the traction unit. For hub motors, their electromagnetic fields are supplied to the stationary windings of the motor. The outer part of the motor follows, or tries to follow, those fields, turning the attached wheel [10].

Based on the space and driving requirement of the original motorcycle, an EVT 900W hub motor with a controller was selected. The maximum speed and torque of the motor is 696 rpm and 25.4 Nm respectively. This motor is a brushed DC motor, and the controller is a PWM controlled MOSFET DC/DC converter. It is important that the controller has following protection strategies: 1) system shutdown when motor temperature above 120°C or controller temperature above 70°C, 2) stop working if the battery terminal voltage lower than 40V, and 3) if the accelerator knob has no action more than 5 minutes, the output will be cut off [11].

Because the hub motor is wider than the original wheel hub, the shock absorber on the motorcycle had to be replaced by a custom fixture. With a tire this hub motor is loaded as the front wheel drive of the HEM as shown in Figure 16.

After installing the motor and controller, the original accelerator handle is replaced by electric accelerator knob. This knob is a variable resistor that determines the pulse width of the motor controller and thus the motor speed can be controlled.

Equation reference goes here HEM system testing

Once the prototype vehicle was constructed, testing was done to validate the functionality of the hybrid system, and determine the fuel economy. Before the whole vehicle test drive was conducted, several subsystem tests were performed to make sure that the subsystems would meet the vehicle's requirements.

HCCI engine subsystem test: In the proposed HEM the HCCI

Figure 16: Hub Motor as Front Wheel Drive Unit.

engine would be managed by a high-level vehicle controller that would (a) automatically switch the engine from SI to HCCI mode (once the in-cylinder temperature and pressure reaches the HCCI threshold), (b) adjust the EGR, and (c) once the engine is in HCCI mode the controller would adjust the generator load to fix the desired engine speed. For the prototype HEM, these events were controlled manually.

The HCCI engine subsystem testing was designed to verify that the modified HCCI engine can operate properly and drive the generator to charge the battery. The testing was also intended to verify that the powertrain would be capable of working well on ECE-40 drive cycle and achieve good fuel economy, once it was integrated into the prototype. A sample of the subsystem testing is shown in Figure 17.

From Figure 17, the engine is first started with SI mode, and the engine speed is adjusted to 3500 rpm by the generator PWM duty cycle. At 25 s, which indicated by the red line, the ECU interface shows that the cylinder head temperature reaches 125°C. At this point the gasoline injection was decreased and the DME injection increased gradually. It can be observed that the engine speed drops below 3500 rpm due to the fuel composition change. The throttle was then opened to 100% and the spark plug was cut off. The combustion mode is thus switched to HCCI and the speed returns to 3500 rpm. Later at 35 s, external EGR is started to help stabilize the combustion. Then the engine is working at stable HCCI state, the speed is fixed at 3500 rpm and the driven generator can output a voltage around 50 V [12-15].

Battery discharge and charge testing: The battery discharge/charge test was conducted to validate the functionality of the charging system, including the DC/DC converter and the charging current control circuit discussed in the previous section. The testing was conducting by driving the HEM on a chassis dynamometer.

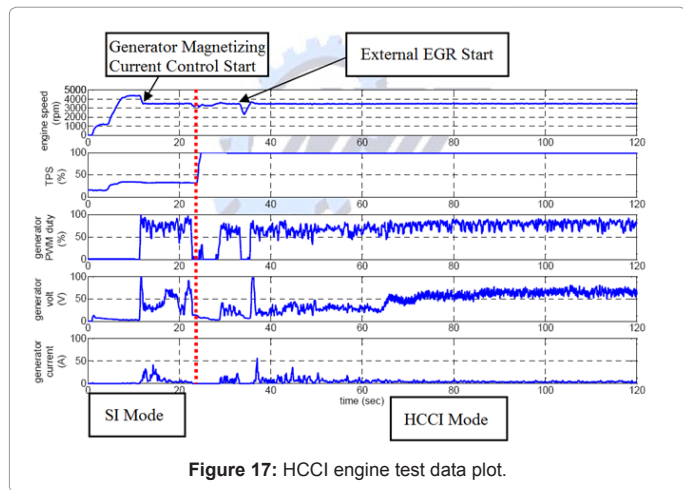Using the battery State-of-Charge (SOC) as a metric for measuring

Figure 17: HCCI engine test data plot.

Data	1st Test	2nd Test	3rd Test	4th Test	5th Test
Initial OCV(V)	50.2	50.2	50.2	50.2	50.2
Discharged OCV (V)	49.96	49.97	49.95	49.96	49.97
Charged OCV(V)	50.07	50.09	50.08	50.07	50.08

Table 3: Single ECE-40 Battery Charging and Discharging OCV.

Data	1st Test	2nd Test	3rd Test	4th Test	5th Test
Initial OCV(V)	50.2	50.2	50.2	50.2	50.2
Final OCV (V)	50.18	50.16	50.19	50.2	50.18
Error Percentage	0.04%	0.08%	0.02%	0%	0.04%

Table 4: Continuous ECE-40 Battery Charging and Discharging OCV.

battery performance was rejected, due to the uncertainty associated with present day SOC estimation methods. Instead, the steady state Open Circuit Voltage (OCV) of the battery was used as a metric. For the purposes of this testing,the battery internal chemical reactions were assumed to reach steady state conditions 30 minutes after a charge or discharge event [d]. By using battery OCV as a metric, the effect of charging or discharging can be estimated reasonably.

Battery testing was conducted in the following manner. First the battery pack was charged to a steady state OCV of 50.2 V. Then the HEM was driven on a chassis dynamometer. To discharge the battery the engine was not started and the HEM was driven for one ECE-40 cycle using only the electrical drive. After a 30 minutes rest the battery OCV was measured to record the 'Discharged OCV'. Subsequently, the vehicle was driven for another ECE-40 cycle, this time with the engine on and running in the HCCI combustion mode. After another 30 minute rest the OCV was measured to record the 'Charged OCV'. Note that during the second cycle, when the engine is running, the generator is not just charging the battery because it is also powering the motor at the same time. This situation represents a real-world working condition for HEM. This test was repeated five times. The results from the testing are shown in Table 3.

From Table 3, the electric-only ECE-40 cycles discharged the battery with an average drop in OCV of 0.24 V. The engine-on ECE-40 cycles increased the OCV by an average of 0.08 V. The results indicate that the engine/generator system is capable of delivering sufficient power to recharge the battery while driving.

With the basic functionality validated, the HEM was tested by driving 6 ECE-40 cycles back-to-back. In this process, the first two cycles were driven in purely electrical drive and the last four cycles were driven with the engine on. Based on the results of single ECE-40 tests the battery OCV should be returned to the initial OCV value at the completion of the six cycles. This series of tests were repeated 5 times and the data is shown in Table 4. Again, the OCV was measured 30 minutes after the test was completed.

From Table 4, the final OCV is reasonably close to initial value with overall error of this testing method being less than 1%. The results indicate that the whole powertrain has no functional obstacles and is capable of meeting the requirements of continuous driving.

Fuel economy test: As mentioned in an earlier section, the fuel economy of the motorcycle was measured in its original configuration (SI engine with CVT transmission) by testing it on a chassis dynamometer. Since motorcycles are typically only driven in normal city traffic the fuel economy was tested using the ECE-40 drive cycle. The test results for the CVT motorcycle are shown in Figure 18.

The CVT motorcycle was driven through six consecutive ECE-40 cycles. By weighting the gasoline consumed, it was determined that the original CVT motorcycle had a fuel economy of 30.8 km/L in city driving.

The fuel economy test for the HEM was conducted in a similar manner, but with the following modification. In the test the HEM runs the first two ECE-40 cycles using pure electric drive, but the engine is running in SI mode to warm it up for switching to HCCI combustion mode. During this time the DC/DC converter is shut down to keep the battery from being charged. Then beginning with the 3rd cycle, the engine is switch on in HCCI mode and the DC/DC converter is turned on to allow the battery to be charged. There are two important points should be noted: 1)because the fuel consumed in SI mode is only for
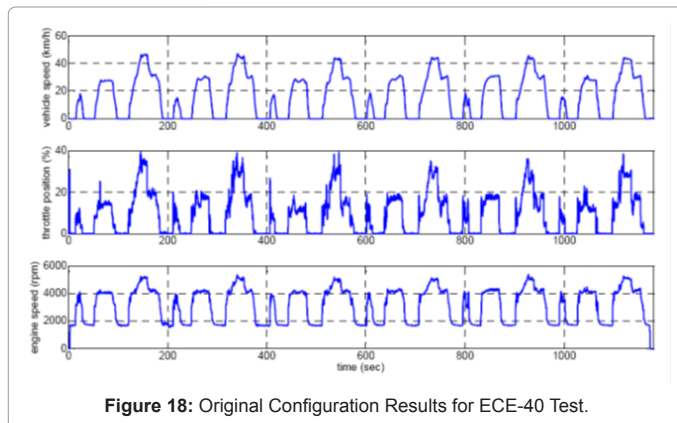
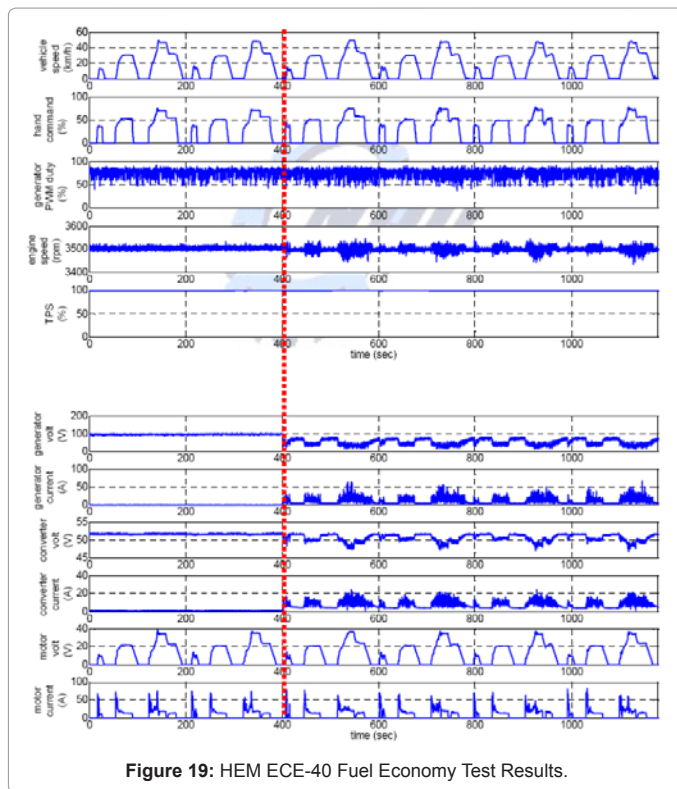**Figure 18:** Original Configuration Results for ECE-40 Test.

Figure 19: HEM ECE-40 Fuel Economy Test Results.

warming the engine and has nothing to do with driving the vehicle, the fuel consumed during this segment was not included in fuel economy calculations and 2) as demonstrated in the battery discharge/charge test, after discharging for two ECE-40 cycles and charging for four cycles, the battery OCV returns back to its initial value. This means that there is no net change in the battery state of charge and the fuel economy calculated during the test is comparable to CVT tests. The test results for the HEM are shown in Figure 19.

As can be seen in Figure 19, during the charging process the engine speed is fixed around 3500 rpm by the generator, which indicates a low BSFC less than 250 g/kWh for this HCCI engine referring to Figure 4. Note that when the battery is being charged (which starts at the red line), the voltage and current output from the generator and DC/DC converter begin to have some ripple. This is because the road load effects are transferred from the wheel motor to the electric system.

During the fuel economy testing of the HEM, both the gasoline and DME consumption were recorded. The mass consumption of the DME was converted to equivalent gasoline mass consumption using the following equation.

$$m_{e,gas} = \frac{m_{DME}H_{DME} + m_{gas}H_{gas}}{H_{gas}}$$

Where $m_{e,gas}$ is the equivalent gasoline mass consumption of DME, m_{DME} and m_{gas} are recorded mass consumption of gasoline and DME in the test, H_{DME} is the Lower Heating Value (LHV) of the DME, which is 28.8 mJ/kg, and H_{gas} is the LHV of gasoline which is 44.4 mJ/kg.

With the recorded data and the results of the previous equation, it was determined that the city driving fuel economy of HEM with the HCCI engine is 73.7 km/L.

Conclusions

This paper discussed a novel powertrain for motorcycle, which combines a HCCI engine in a series hybrid configuration. The prototype vehicle developed here has very good functionality. The modified engine can be switched from SI mode to HCCI very smoothly, and works stably in HCCI mode with external EGR. During HCCI mode operation, the engine speed is fixed at 3500 rpm, with a BSFC less than 250 g/kWh. The electricity generated in HCCI working mode is capable of charging the 48V battery at a constant rate of 5A. Overall, the city driving fuel economy of the motorcycle is increased from 30.8 km/L to 73.7 km/L which is a 139% improvement. The experimentally measured values were with 10% of the values predicted by the mathematical models (32.6 km/L and 75.6 km/L), which validates the numerical models.

The testing conducted here indicates that a HCCI engine in a series hybrid configuration holds tremendous promise for improving fuel economy. The present prototype still has potential for improvement. Developing a method to automatically switch to HCCI combustion mode will be pursued in the future. Also implementing a SOC estimation scheme combined with engine start control will make this powertrain more intelligent and efficient [16,17].

Acknowledgement

References

1. World Energy Outlook 2012, International Energy Agency.

2. International Energy Outlook 2011, U.S. Energy Information Administration, Report DOE/EIA-0484(2011), September 2011.

3. Kang H (2007) An Analysis of Hybrid-Electric Vehicles as the Car of The Future: Bachelor Thesis, Massachuset Institute Of Technology.

4. Dec JE (2009) Advanced Compression-Ignition Engines-Understanding the In-Cylinder Processes: Proceedings of the Combustion Institute (32) 2727-2742

5. Sun R, Thomas R, Gray CL (2004) An HCCI Engine: Power Plant for a Hybrid Vehicle: SAE Paper No. 2004-01-0933.

6. Bing-Feng Liu, Yuh-Yih Wu, Ta-Chiuan Liu (2010) "Operation Range Expansion of HCCI Engine Using Mixed Fuel And EGR". The 15th National Conference on Vehicle Engineering, Tainan, Taiwan.

7. ADVISOR (Advancedvehiclesimulator) Software: U.S. Department Of Energy's National Renewable Energy Laboratory's (NREL) Center For Transportation Technologies And Systems.

8. Yuh-Yih Wu, Hsien-Chi Tsai, Ta-Chiuan Liu (2010) Investigation of Running HCCI with Dual-Fuel in a Small Scale Engine. ASME International Combustion Engine Division 2010 Fall Technical Conference, San Antonio, TX, USA.

9. Kai-Xian Hong (2011) "Investigation", Master Thesis, National Taipei University of Technology.

10. Turns SR (2012), An Introduction to Combustion: Concepts and Applications: Mcgraw-Hill,2012.

11. Omar N, Mierlo JV, Verbrugge B, Bossche PV (2010) Power And Life Enhancement Of Battery-Electrical Double-Layer Capacitor For Hybrid Electric And Charge-Depleting Plug-In Vehicle Applications: Electrochimicaacta 55: 7524-7531.

12. Hegazy O, Mierlo JV, Barrero R, Omar N, Lataire PH (2013) PSO Algorithm-Based Optimal Power Flow Control of Fuel Cell / Supercapacitor and Fuel Cell/ Battery Hybrid Electric Vehicles: J Comp and Math In Elect and Elect Eng 32: 86-107.

13. Omar N, Daowd M, Hegazy O, Bossche PV, Coosemans TH, et al (2010) Electrical Double-Layer Capacitors In Hybrid Topologies-Assessment and Evaluation of the Performances Energies 55: 7524-7531.

14. Lawler B, Ortiz-Soto E, Gupta R, Peng H, et al (2011) Hybrid Electric Vehicle Powertrain And Control Strategy Optimization To Maximum The Synergy With Gasoline HCCI Engine: SAE Int J Engines 4: 1115-1126.

15. Sun R, Patrick R, Tang X (2012) HCCI Engine Application on a Hydraulic Hybrid Bus: SAE 2012 International Powertrains, Fuels and Lubricants Meeting 5: 1581-1594.

16. Masato I, Yuichiro K, Norimasa I (2005) Development of a Control System Using EGR Gas for HCCI Engine Running on DME: Transaction of SAE Japan 40: 13-18.

17. Mingfa Y, Chen Z, Zunqing Z, Zhang B, Xing Y (2006) Effect Of EGR On HCCI Combustion Fuelled With DME And Methanol Dual-Fuels: Powertrains And Fluid Systems Conference & Exhibition.